

Study on the RC Frame with the Partial Infill Wall in Pushover Analysis

Mo Shi¹, Xiaoyan Xu² and Yeol Choi^{1,*}

¹School of Architectural Engineering, Kyungpook National University, Daegu, South Korea

²Chief Executive Officer, HaXell elevator, Shanghai, China

* Corresponding Author

Abstract

The short column effect is a major contributor to structural failure during seismic events. However, while most investigations concentrate on its influence on external walls, it also causes damage to interior walls. This underscores the significance of exploring interior wall damage due to this effect. This study involves four variations of RC frames with infill walls, analyzed using the Pushover method within the SAP 2000 software. The Pushover analysis vividly portrays the behavior and performance of interior wall systems. A comprehensive comparison of metrics like base shear, column shear force, and plastic hinge behavior underscores the pivotal role of interior walls in the entire structure, accentuating the necessity of delving into interior wall research.

Keywords

Short Column Effect; Infill Wall; SAP 2000.

1. Introduction

The 2017 earthquake in Pohang City, Republic of Korea, left a profound impact, resulting in considerable casualties and substantial economic damage. The unexpected nature of this event spurred comprehensive research into its structural consequences. Scholars extensively simulated the earthquake's behavior, and the study "Development of Simulation Model for the 2017 Pohang Earthquake and Construction of Hazard Map based on its Scenario" by Jee, Hyun Woo, and Han, Sang Whan provided amplification factor values for the Korean Peninsula, as illustrated in Figure 1.

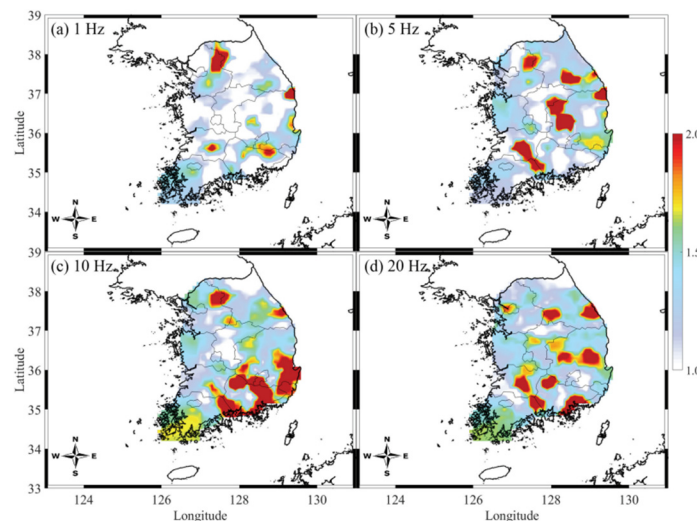


Figure 1. Estimated Site Amplification Factor Values for the Korea Peninsula at Each Frequency

The findings from the Pohang earthquake research enable the development of well-suited earthquake-proof and earthquake-resistant structures, along with effective reinforcement strategies. By integrating the latest advancements in this domain, these insights serve as essential guidelines for construction endeavors.

Moreover, subsequent to the Pohang Earthquake, other researchers conducted direct assessments of the earthquake's aftermath. While structural collapses occurred for multiple reasons, specific instances of failure were linked to the short column effect, as depicted in Figure 2, as evidenced in "Building Damage in Pohang EQ and the Lessons, 2018/12, Park, Hong-Gun; Park, Hong-Gun."

Illustrated in Figure 2 and the publication "Building Damage in Pohang EQ and the Lessons, 2018/12, Park, Hong-Gun; Park, Hong-Gun," the author examines the repercussions of earthquake-induced shaking, emphasizing instances of short column failure within RC frames equipped with infill wall systems. This type of structural failure is notably prevalent in educational buildings.



Figure 2. Shear Failures on Short Column effect

While the majority of research has addressed damage to RC frames with external wall systems and the short column effect, the need to explore interior infill wall systems' impact on seismic damage becomes evident. This study focuses on four distinct types of RC frames with interior infill walls, designed based on the structure of Kyungpook National University's Department of Architectural Engineering building (No.401). Employing Pushover Analysis, this study examines the earthquake behavior and performance of these structures. By comparing parameters like base shear force, shear force, and plastic hinge behavior on columns, the safety of RC frames with interior wall systems is assessed. The study offers preliminary insights for reinforcing RC frames with interior infill walls, aiming to reduce the economic losses and casualties arising from earthquake-induced damage.

2. Structure Description and Load Design

2.1. Structure Description

This research centers on the analysis of an educational building dating back to the 1970s, specifically targeting No.401 within Kyungpook National University's Department of Architectural Engineering, situated in Daegu Metropolitan City, Republic of Korea. The study scrutinizes the conventional layout of the RC frame as displayed on the building's ground plan, while the cross-section reveals unique openings designed for high windows and doors.

Drawing from the cross-section, the presence of a high window and door opening is apparent in room No.119. This specific room is selected as the primary subject of this study, as designated on the building's ground plan. The configuration of room No.119 is visually represented in Figure 3.

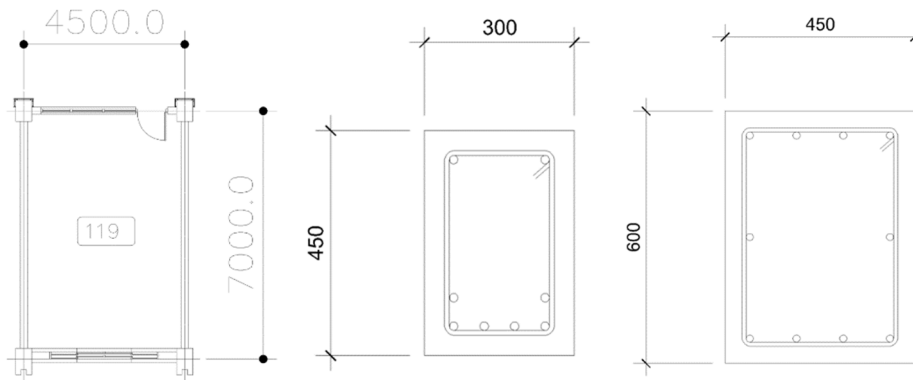


Figure 3. Layout plan
(Room No.119 / Column Section / Beam Section)

Furthermore, Figure 3 offers cross-sectional depictions of both the column and beam, while Table 1 outlines the respective designs for these integral components.

Table 1. Design of column and beam

Concrete	Weight per unit volume		23.54 kN/m ³	
	Mass per unit volume		2.4004 kN/m ³	
	Modulus of elasticity		22334 MPa	
	Poisson		0.1667	
	Coefficient of Thermal expansion		1.100E-05	
	Specified Compressive Strength		15.12 MPa	
	Expected Compressive Strength		18.14 MPa	
Rebar	Weight per unit volume		77 kN/m ³	
	Mass per unit volume		7.85 kN/m ³	
	Modulus of elasticity		200000 MPa	
	Poisson		0.3	
	Coefficient of Thermal expansion		1.170E-05	
	Minimum Stress		240 MPa	
	Expected Stress		300 MPa	
Column	Longitudinal Rebar	8-D19 & 2-D16	Stiffness of Shear	0.45
	Hoop Rebar	D10@300	Stiffness of Moment	0.70
Beam	Longitudinal Rebar	8-D16	Stiffness of Shear	0.45
	Hoop Rebar	D10@300	Stiffness of Moment	0.35

The infill wall characteristics adhere to the specifications presented in Table 2 of KS L 4201:2020 (Clay brick), a choice guided by the educational building design directives of the Ministry of Education of the Republic of Korea in the 1980s. Moreover, in line with KISTEC 2021's Table 5.3.1, shear stiffness is defined as 0.4, while moment stiffness is established at 0.35, reflecting the traits typical of school structures from the 1980s.

Drawing from the layout plan of room No.119 displayed in Figure 3, the design of analytical specimen structures is depicted in Figure 4. While maintaining a consistent infill wall height (Door Height: 2350mm) within the RC frame, the variable lies in the width of the high window segment. Notably, this excludes the fundamental structure lacking an infill wall.

Table 2. Design of infill wall

Material Properties	Weight per unit volume	16 kN/m ³
	Mass per unit volume	1.6315 kN/m ³
	Modulus of elasticity	420 MPa
	Poisson	0.25
	Coefficient of thermal expansion	1.000E-05
	Shear Modulus	168 MPa
	Specified Compressive Strength	2.1 MPa
	Expected Compressive Strength	2.73 MPa
Specifications	Length	240(mm) ± 2.0(mm)
	Width	115(mm) ± 1.5(mm)
	Height	53(mm) ± 1.5(mm)
	Stiffness of Shear	0.4
	Stiffness of Moment	0.35

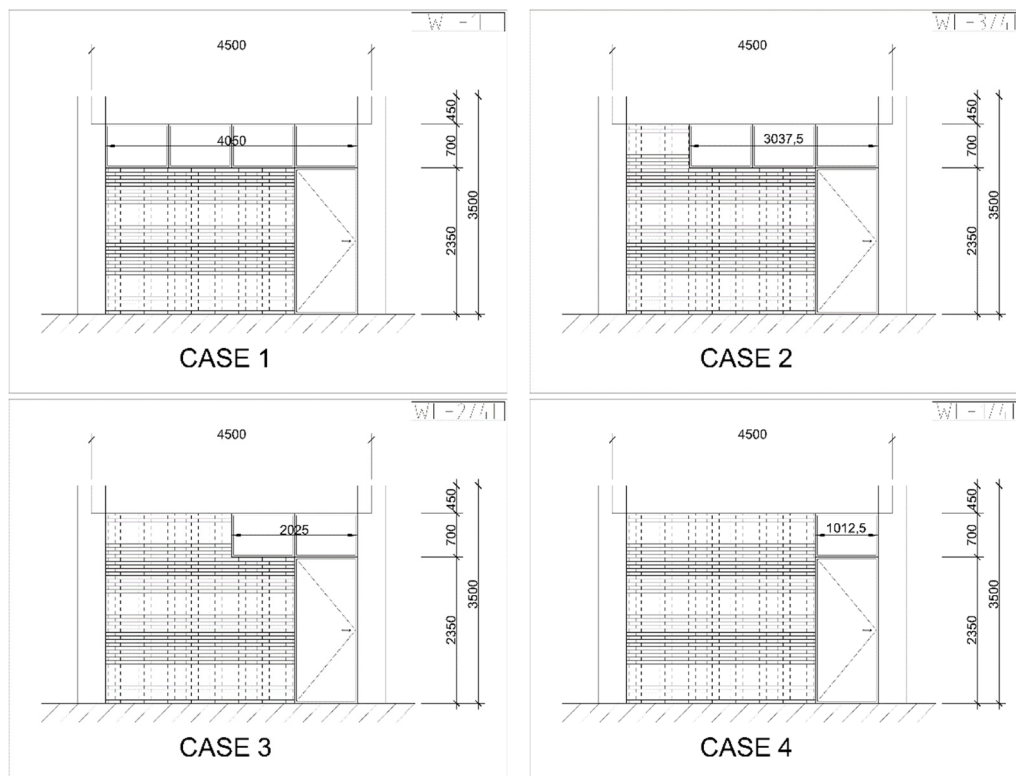


Figure 4. Design of analytical specimen

2.2. Plastic Hinge Design

The Response Spectrum analysis outcomes guide the design of plastic hinges, aligning with the ASCE 41-13 standard recommended by SAP 2000, for each yield moment corresponding to the structure's plastic hinges.

Plastic hinges for columns are formulated in accordance with ASCE 41-13 Table 10-8 (Concrete Columns), specifically Condition ii-Flexure/Shear. Concurrently, plastic hinges for beams adhere to ASCE 41-13 Table 10-7 (Concrete Beams-Flexure), item i, relating to the flexural characteristics of concrete beams within the RC frame.

2.3. Load Design

2.3.1. Dead Load & Live Load Design

Based on KBC 2016, the Dead Load and Live Load for the school building's educational usage are indicated as 4.3kN/m² and 3kN/m², respectively. This information is presented in Table 0303.2.1 of KBC 2016.

Subsequently, by taking into account the dimensions of room No.119, the calculations for the Dead Load and Live Load can be performed using the formulas provided below:

$$\omega_D = P_D / L. \tag{1}$$

$$\omega_L = P_L / L. \tag{2}$$

Where P_D represents the Dead Load force, and ω_D signifies the uniform load from the Dead Load. Conversely, P_L denotes the Live Load force, and ω_L represents the uniform load from the Live Load. Utilizing these calculations, the Dead Load is ascertained to be 4.83751kN/m, and the Live Load is calculated to be 3.375kN/m.

2.3.2. Response Spectrum

Based on KISTEC 2021, the analysis of the target structure through response spectrum methodology involves the utilization of the response spectrum presented in Figure 9, which is sourced from KBC 2016.

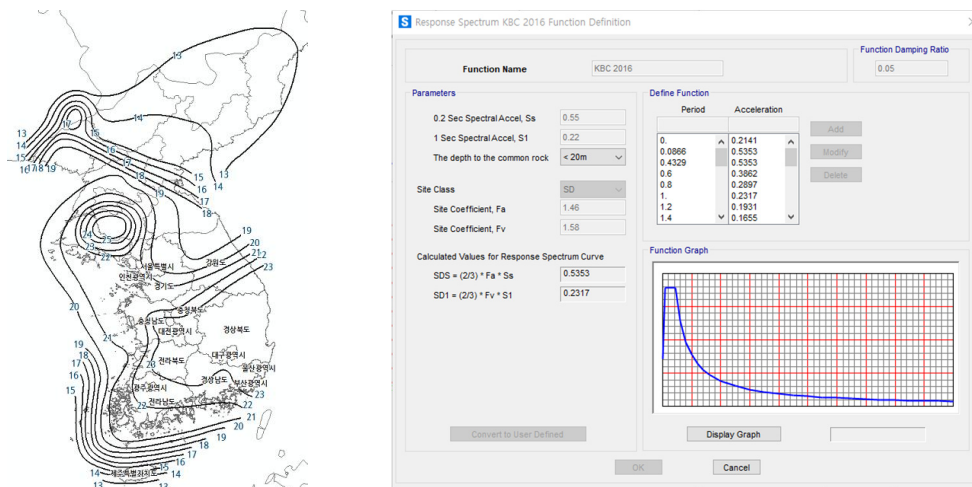


Figure 5. Earthquake hazard map and Response spectrum

In line with KBC 2016, Figure 5 portrays the earthquake hazard map of the Republic of Korea on the left. This map is then used to define the response spectrum, categorized as site class SD, based on the location of the research's target building, No.401, situated at Kyungpook National University's Department of Architectural Engineering in Daegu Metropolitan City. The Figure 5 depiction on the right side showcases the corresponding response spectrum for SD classification.

Utilizing the equation provided by KBC 2016, the computation of both the 1-sec spectral acceleration and the 0.2-sec spectral acceleration becomes feasible.

$$S_{D1} = S \times F_v \times 2/3. \tag{3}$$

$$S_{DS} = S \times 2.5 \times F_a \times 2/3. \tag{4}$$

Where S represents the effective ground acceleration value for a 2400-year return period earthquake, sourced from Table 0306.3.1 of KBC 2016. Additionally, the factors F_a and F_v , found in Table 0306.3.3 and Table 0306.3.4 respectively as per KBC 2016, play a role. Using these parameters, the calculations yield S_{D1} for the 1-sec spectral acceleration and S_{D5} for the 0.2-sec spectral acceleration. Applying the provided equations, the 1-sec spectral acceleration is computed as 0.22g, while the 0.2-sec spectral acceleration stands at 0.55g. These results are also visually represented on the right side of Figure 5.

2.3.3. Pushover Analysis

According to KISTEC 2021, the load combination for Pushover analysis is presented in the following formula:

$$\text{Load combination} = 1.0 \times (\text{Dead Load}) + 0.25 \times (\text{Live Load}). \tag{5}$$

Moreover, the pushover analysis employs a displacement control system utilizing conjugate displacement for controlling the process. The consideration involves the provision of detailed data as the calculation progresses, this analysis is structured across 100 steps totally, each characterized by distinct displacement values.

3. Discussion of Response Spectrum Analysis

As depicted in Figure 6, a notable observation is that the RC frame without an infill wall consistently displays higher moment values compared to the RC frame with an infill wall. When examining different cases, ranging from CASE-1 to CASE-4, a consistent upward trend is evident in the moment values of the left column. On the contrary, the moment outcomes for the right column of the structure display relatively minor discrepancies. This comparable pattern is also witnessed in the beam section, mirroring the observations from the right column.

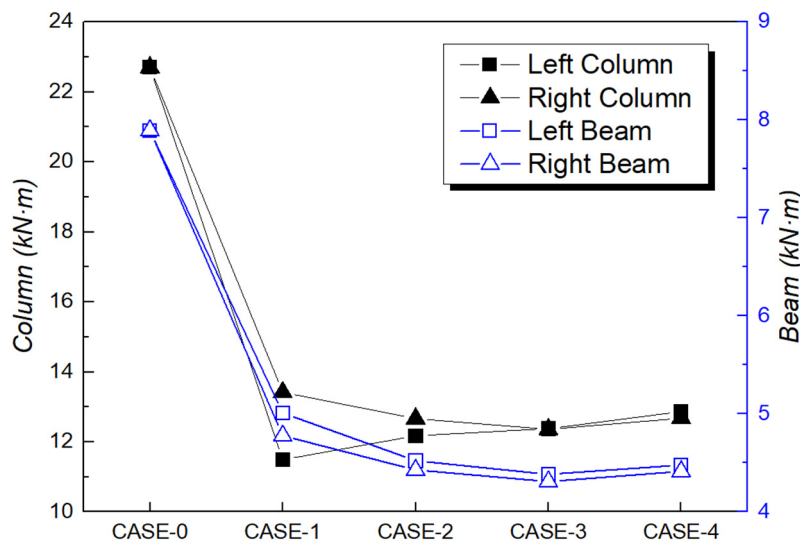


Figure 6. Moment result under the response spectrum analysis

The shear force outcomes present a striking contrast to the moment results, as demonstrated in Figure 7. Although the RC frame lacking an infill wall continues to display higher shear force values than the one with an infill wall, an atypical behavior arises from the left column of the structure, especially within the column element connected to the infill wall.

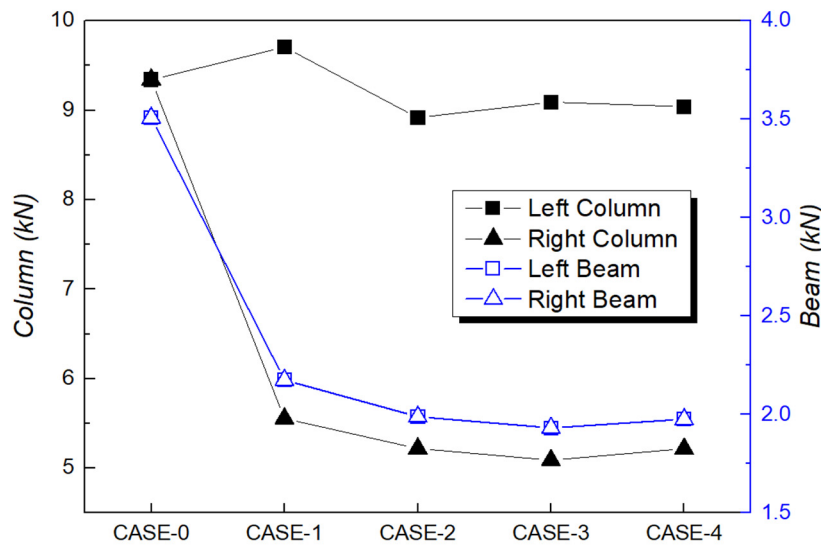


Figure 7. Shear force result under the response spectrum analysis

As depicted in Figure 7, the greatest shear force is observed in CASE-1, corresponding to a 2350mm infill system height. As the infill wall's height increases, the shear force experiences a significant reduction. Nevertheless, with the augmentation of the horizontal extent of the infill wall, the shear force shows a gradual increase. Specifically comparing CASE-1 and CASE-4, isolating the effect of horizontal infill wall extension, the lesser shear force is identified at a 3050mm infill wall height.

4. Discussion of Pushover Analysis

4.1. Performance Point

The findings in Table 3 display the performance points for various scenarios utilizing FEMA 440 Equivalent Linearization. It's evident that the absence of an infill wall in the RC frame leads to reduced shear force and displacement. A comparison between CASE-1 and CASE-4, independent of horizontal infill wall expansion, reveals that higher infill wall heights are associated with significantly elevated shear forces and accompanying displacement. Notably, CASE-2 records the utmost displacement, suggesting that the expansion of the infill wall's horizontal area also influences performance point outcomes.

Table 3. Performance Point

Type	V	D	Sa	Sd	Tsec	Ductility	Beff	M
	kN	mm	g	mm	sec	Unitless	Unitless	Unitless
CASE-0	18.933	1.314	0.539	1.304	0.098	2.445	0.119	1.3
CASE-1	30.266	1.655	0.704	1.313	0.087	4.583	0.201	2.022
CASE-2	47.952	2.027	0.946	1.567	0.082	6.436	0.205	2.824
CASE-3	47.737	1.895	0.899	1.433	0.08	5.988	0.205	2.714
CASE-4	50.523	2.004	0.919	1.497	0.081	6.117	0.205	2.758

Analyzing the Sa (Spectral acceleration) and Sd (Spectral displacement) outcomes, it's evident that the RC frame lacking an infill wall exhibits decreased shear force and displacement. Interestingly, CASE-2 presents the maximum result, indicating a departure from the preceding cases. When considering the range from CASE-1 to CASE-4 and the variations in infill wall height,

it becomes apparent that infill wall height predominantly impacts the performance points during pushover analysis.

The period (Tsec) results in Table 3 display a lengthier period (0.098 sec) for CASE-0, corresponding to the RC frame devoid of an infill wall. As infill wall height escalates within the RC frame, periods decrease. In the comparison between CASE-1, CASE-2, CASE-3, and CASE-4, it becomes evident that infill wall height exerts a more substantial influence on the structure than the extension of its horizontal area.

4.2. Discussion of Capacity Curve

Illustrated in Figure 8, the capacity curve analysis shows distinct behaviors. Contrasting the RC frame with and without an infill wall, the former displays reduced displacement yet increased base force. Additionally, taller infill walls result in briefer displacement and augmented base shear. Observing the curves of the RC frame with an infill wall, it becomes evident that extending the wall horizontally at the same height has a comparatively lesser effect on the overall structural performance, unlike the notable influence of the wall's height.

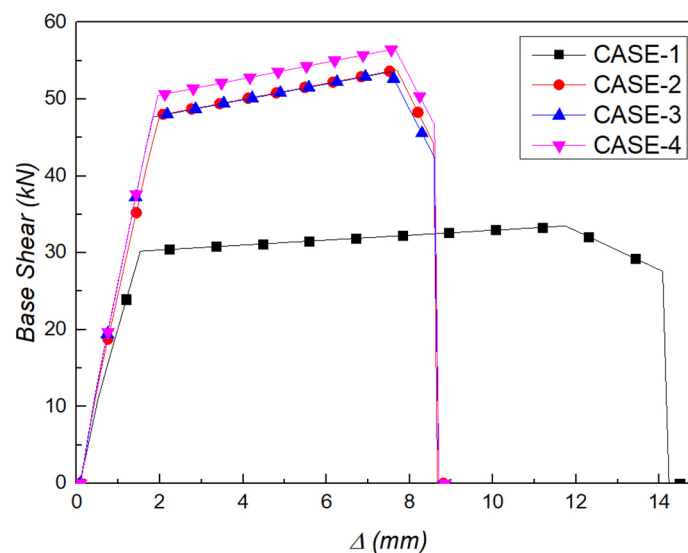


Figure 8. Capacity Curves

4.3. Discussion of Yield and Collapse Points

The yield and collapse points of the structures are detailed in Table 4, showcasing significant distinctions between the RC frame with and without an infill wall system. Notably, at the yield point, the RC frame lacking an infill wall demonstrates extended displacement and reduced base force, while at the collapse point, this difference becomes even more pronounced, with the RC frame without an infill wall exhibiting both longer displacement and lower base force in contrast to the infill wall equipped frame.

When assessing the RC frame with an infill wall system, it's noticeable that elevating the infill wall's height corresponds to lengthier displacements (CASE-1 & CASE-4). Conversely, the gradual reduction in displacement occurs with the horizontal extension of the infill wall (CASE-2, CASE-3, and CASE-4). In terms of base force, taller infill walls result in increased base forces (CASE-1 & CASE-4), and extending the infill wall horizontally doesn't lead to a distinct difference in alteration.

The results at the collapse point mirror those seen at the yield point. As indicated in Table 4, the contrast between the RC frame without an infill wall and the RC frames with an infill wall is observable. Especially, it's apparent that altering the horizontal extension of the infill wall, while maintaining the same height, has a relatively smaller impact on the overall structural performance in comparison to the influence of adjusting the height of the infill wall.

Table 4. Yield & Collapse Points

Type	Yield Points		Collapse Points	
	Displacement	Base Force	Displacement	Base Force
	mm	kN	mm	kN
CASE-0	3.027174	22.155	58.582419	23.806
CASE-1	1.529329	30.226	11.749329	33.498
CASE-2	2.081524	48.009	7.691524	53.788
CASE-3	1.837584	47.678	7.532584	53.549
CASE-4	1.953371	50.469	7.648371	56.543

5. Conclusion

Derived from FEMA 440 Equivalent Linearization, the Pushover analysis reveals heightened shear force and extended displacement with increased infill wall height. Similarly, taller infill walls correlate with higher spectral acceleration (S_a) and more extensive spectral displacement (S_d), while exhibiting shorter period (T_{sec}). Nonetheless, findings from CASE-2 to CASE-4 closely resemble those of the Response Spectrum analysis, indicating limited disparities in the impact of various horizontal extensions of the infill wall under the same height.

The yield point analysis of plastic hinges highlights a significant contrast between the RC frame and those incorporating an infill wall system. Notably, the RC frame lacking an infill wall displays lengthier displacement and decreased base shear force. Contrasting this with the RC frame having an infill wall, taller infill walls correspond to elevated base shear forces, while altering the wall's horizontal extension has minimal influence on base shear force. Similar trends are noted in the behavior of displacement. These consistent patterns extend to observations at the collapse point as well.

In conclusion, this study investigates the influence of infill wall height on the structural behavior of high window structures commonly found in Korean educational buildings. The research reveals that the vertical height of the infill wall significantly impacts the RC frame's performance, while its horizontal extension has minimal effect. To prevent potential collapse stemming from the short column effect, constructing taller infill walls with proportionally shorter horizontal extensions emerges as a prudent strategy for these distinctive high window structures.

Acknowledgments

This work was supported by the Shanghai HaXell elevator.

References

- [1] Hyun.Woo. Jee, Sang.Whan. Han: Development of Simulation Model for the 2017 Pohang Earthquake and Construction of Hazard Map based on its Scenario, Magazine of The Korean Society of Hazard Mitigation, vol. 19 (2019), 289-301.
- [2] Hong.Gun. Park, Chul.Goo. Kim: Building Damage in Pohang EQ and the Lessons, Review of Architecture and Building Science, vol. 62 (2018), 64-67.
- [3] Gao. Ma, Hui. Li, Hyeon.Jong. Hwang: Seismic behavior of low-corroded reinforced concrete short columns in an over 20-year building structure, Soil Dynamics and Earthquake Engineering, vol. 106 (2018), 90-100.
- [4] Beom.Seok. Kim, Ji.Hun. Park: Response Modification Factors of Non-seismic School Buildings Considering Short Column Effects and Natural Period, Earthquake Engineering Society of Korea, vol. 23 (2019), 71-82.

- [5] Ismail.H. Cagatay, Caner. Beklen, Khalid. M. Mosalam: Investigation of short column effect of RC buildings: failure and prevention, *Computers and Concrete*, vol. 7 (2010), 523-532.
- [6] Xiao.Jie. Zhou, Xiao.Yuan. Kou, Quan.Min. Peng, Jin.Tao. Cui: Influence of Infill Wall Configuration on Failure Modes of RC Frames, *Hindawi*, vol. 2018 (2018), 1-14.
- [7] Reshma.B. Philip, Manoj.C. M: Effect of Short Column Behavior on the Seismic Performance of a Reinforced Concrete Structure on Sloping Lot, *International Journal of Engineering Research & Technology (IJERT)*, vol. 6 (2018), 1-5.
- [8] A.B.M.A. Kaish, M.R. Alam, M. Jamil, M.F.M. Zain, M.A. Wahed: Improved ferrocement jacketing for restrengthening of square RC short column, *Construction and Building Materials*, vol. 36 (2012), 228-237.
- [9] Helmut. Krawinkler, G.D.P.K. Seneviratna: Pros and cons of a pushover analysis of seismic performance evaluation, *Engineering Structures*, vol. 20 (1998), 452-464.
- [10] Liu. Jin, Min. Du, Dong. Li, Xiu.Li. Du, Hai.Bin. Xu: Effects of cross section size and transverse rebar on the behavior of short squared RC columns under axial compression, *Engineering Structures*, vol. 142 (2017), 223-239.
- [11] Shuang. Li, Zhan.Xuan. Zuo, Chang.Hai. Zhai, Li.Li. Xie: Comparison of static pushover and dynamic analyses using RC building shaking table experiment, *Engineering Structures*, vol. 136 (2017), 430-440.
- [12] Reza. Karimi, Mehrzad. TahamouliRoudsari: Quasi-static cyclic testing of RC frames retroftted using steel plate shear walls and diagonal tensile mesh, *Asian Journal of Civil Engineering*, vol. 22 (2021), 1301-1318.